

play an important role in the models of atmosphere emission from strongly magnetized neutron stars.^{13,14} Both processes are very important in the models of the radiation emission during SGR burst.^{6,15,16}

Previously, Compton scattering was studied under various conditions. The case of the magnetic field without plasma was investigated.^{17,18} It was found that Compton scattering becomes strongly anisotropic and essentially depends on photon polarization. It was shown¹⁴ that the dispersion properties of photon in strongly magnetized cold plasma could significantly influence on the process under consideration.

In the present work the process of photon scattering, $e\gamma \rightarrow e\gamma$, is investigated in the presence of strong magnetic field and electron-positron plasma, when the magnetic field strength B is the maximal physical parameter, namely $eB \sim T, \mu_{e\pm}, E$. Here T is the plasma temperature, $\mu_{e\pm}$ is the chemical potential, and E are the initial photon and electron (or positron) energies. In this case almost all electrons and positrons in plasma are on the ground Landau level. We also consider the nonresonance case, when electron and photon momenta satisfy the condition $eB \gg (pq) + q^2/2$ (the quantities (pq) and q^2 are defined in Sec. 2). Such conditions could be realized, e.g. in the Thompson and Duncan model of SGR burst⁶ where the creation of magnetically trapped high temperature (~ 1 MeV) plasma in the ball is assumed or in the outer crust of magnetar in not too dense degenerate plasma.²¹

The main purposes of our work are: to investigate the influence of the strongly magnetized plasma on the process of Compton scattering taking account of photon dispersion and wave function renormalization and to compare the Compton scattering with the process of photon splitting.

The paper is organized as follows. In Sec. 2 we consider the propagation of the electromagnetic radiation in magnetized medium and give the expression of Compton scattering amplitudes for different polarization configurations of the initial and final photons. The analytic and numerical calculations of the photon absorption rate and cross-section of the process are presented in Sec. 3. The discussion of the possible astrophysical application of Compton scattering are given in Sec. 4.

2. Photon Propagation in Strongly Magnetized Plasma

The propagation of the electromagnetic radiation in any active medium is convenient to describe in terms of normal modes (eigenmodes). In turn, the polarization and dispersion properties of normal modes are connected with eigenvectors and eigenvalues of polarization operator correspondingly. In the case of strongly magnetized plasma when the electrons and positrons are on the ground Landau level (i.e. effectively one-dimensional) in the one-loop approximation the eigenvalues of the polarization operator can be derived from the previously obtained results:^{22,24}

$$P^{(1)}(q) = i\frac{e^2}{6} \frac{q^2}{q^2 + \frac{(6N_e)^2 q^2}{q^2}} \mathcal{P}_0(q^2, B), \quad (1)$$

$$P^{(2)}(q) = \frac{2eB}{i\sqrt{2}\omega_0} H \frac{q^2}{4m^2} + J(q) \sqrt{\omega_0 q^2} (B), \quad (2)$$

$$P^{(3)}(q) = \frac{2eB}{i\sqrt{2}\omega_0} q^2 \sqrt{\omega_0} \sqrt{q^4 + \frac{(6N)^2 q^2}{q^2}} \sqrt{\omega_0 q^2} (B), \quad (3)$$

where

$$(B) = \frac{1}{3} 1.792 \sqrt{\omega_0} \ln \frac{B}{B_e}, \quad N = \int_{\omega_0}^{\infty} dp_z [f_{\omega_0}(E) \sqrt{\omega_0} f_+(E)],$$

$$J(q) = 2q^2 m^2 \frac{dp_z}{E} \frac{f_{\omega_0}(E) + f_+(E)}{(q^2)^2 \sqrt{\omega_0} (pq)^2}, \quad E = \sqrt{p_z^2 + m^2},$$

$f_{\omega_0}(E) = [e^{(E\sqrt{\omega_0})/T} + 1]^{-1}$ are the electron (positron) distribution functions,

$$H(z) = \frac{1}{z(1\sqrt{\omega_0 z})} \arctan \frac{z}{1\sqrt{\omega_0 z}} \sqrt{\omega_0}, \quad 0 \leq z \leq 1, \quad (4)$$

$$H(z) = \frac{1}{2} \frac{1}{z(z\sqrt{\omega_0})} \ln \frac{\bar{z} + \frac{z\sqrt{\omega_0}}{z\sqrt{\omega_0}}}{\bar{z}\sqrt{\omega_0} \frac{z\sqrt{\omega_0}}{z\sqrt{\omega_0}}} \sqrt{\omega_0} + \frac{i}{2} \frac{1}{z(z\sqrt{\omega_0})}, \quad z > 1. \quad (5)$$

In the case of strongly degenerate plasma ($T \ll \omega_0$) one can obtain the analytical expressions for $J(q)$ and N integrals:

$$J(q) = \frac{1}{2} \frac{1}{z(1\sqrt{\omega_0 z})} \arctan \frac{v_F \sqrt{\omega_0} + z v_F (v^2 \sqrt{\omega_0})}{(v^2 \sqrt{\omega_0}) \sqrt{z(1\sqrt{\omega_0 z})}} + \arctan \frac{v_F + v + z v_F (v^2 \sqrt{\omega_0})}{(v^2 \sqrt{\omega_0}) \sqrt{z(1\sqrt{\omega_0 z})}}, \quad 0 \leq z \leq 1, \quad (6)$$

$$J(q) = \frac{1}{4} \frac{1}{z(z\sqrt{\omega_0})} \ln \frac{v_F \sqrt{\omega_0} + (v^2 \sqrt{\omega_0}) \sqrt{z v_F \omega_0} \sqrt{z(z\sqrt{\omega_0})}}{v_F \sqrt{\omega_0} + (v^2 \sqrt{\omega_0}) \sqrt{z v_F \omega_0} \sqrt{z(z\sqrt{\omega_0})}} + \ln \frac{v_F + v + (v^2 \sqrt{\omega_0}) \sqrt{z v_F \omega_0} \sqrt{z(z\sqrt{\omega_0})}}{v_F + v + (v^2 \sqrt{\omega_0}) \sqrt{z v_F \omega_0} \sqrt{z(z\sqrt{\omega_0})}} \quad (7)$$

$$\frac{i}{2} \frac{1}{z(z\sqrt{\omega_0})} \frac{(v_F/v + i\sqrt{\omega_0})}{z(z\sqrt{\omega_0})}, \quad z > 1,$$

$$z = \frac{q^2}{4m^2}, \quad v_F = \frac{\sqrt{\omega_0 \omega_0} m^2}{\omega_0}, \quad v = \frac{q}{q_z}, \quad N = 2p_F = 2 \sqrt{\omega_0 \omega_0} m^2.$$

Here the four-vectors with indices μ and ν belong to the Euclidean $\{1, 2\}$ -subspace and the Minkowski $\{0, 3\}$ -subspace correspondingly in the frame where the magnetic field is directed along z (third) axis; $(ab) = (a \cdot b) = a \cdot b$, $(ab) =$

$(a \sim b) = a \sim b$, where the tensors $\epsilon_{\alpha\beta} = (\epsilon_{\alpha\beta})$, $\tilde{\epsilon} = (\tilde{\epsilon})$, with equation $\tilde{\epsilon} \epsilon_{\alpha\beta} = g = \text{diag}(1, \epsilon_{\parallel 1}, \epsilon_{\parallel 1}, \epsilon_{\parallel 1})$ are introduced. $\epsilon_{\parallel 1} = F/B$ and $\tilde{\epsilon} = \frac{1}{2} \epsilon_{\alpha\beta} \epsilon_{\alpha\beta}$ are the dimensionless $\epsilon_{\parallel 1}$ tensor and dual $\epsilon_{\parallel 1}$ tensor correspondingly.

The dispersion properties of the normal modes can be defined from the dispersion equations

$$q^2 \epsilon_{\alpha\beta}^{(1)}(q) = 0 \quad (\alpha = 1, 2, 3). \quad (8)$$

Their analysis shows that 1 and 2 modes with polarization vectors

$$^{(1)}(q) = \frac{(q)}{q^2}, \quad ^{(2)}(q) = \frac{(q)}{q^2} \quad (9)$$

are only physical ones in the case under consideration, just as it is in the pure magnetic field. However, it should be emphasized that this coincidence is approximate to within $O(1/eB)$ and $O(\epsilon^2)$ accuracy.

We notice that in plasma only the eigenvalue $P^{(2)}(q)$ is modified in comparison with pure magnetic field case. It means that the dispersion law of the mode 1 is the same one as in the magnetized vacuum, where its deviation from the vacuum law, $q^2 = 0$, is negligibly small. On the other hand, the dispersion properties of the mode 2 essentially differ from the magnetized vacuum ones. In Figs. 1 and 2 the photon dispersion in both strong magnetic field and magnetized plasma are depicted at various temperatures (for the charge-symmetric plasma) and chemical potential (for the degenerate plasma). One can see that in the presence of the magnetized plasma there exist the kinematical region, where $q^2 > 0$ contrary to the case of pure magnetic field. It is connected with the appearance of the plasma frequency in the presence of the real electrons and positrons which can be defined from equation

$$\epsilon_{\parallel 1}^{(2)}(q_{\parallel}, \mathbf{k} = 0) = 0. \quad (10)$$

This fact can lead to the modification of the kinematics of the different processes with photons. For example, the photon splitting channel $\gamma \rightarrow \gamma + \gamma$ forbidden in the magnetic field without plasma becomes allowed. ²⁶

Moreover, as can be seen from Fig. 2 in degenerate plasma there is to be the shift of the e^+e^- pair-creation threshold which in pure magnetic field is defined by the relation $q^2 = 4m^2$. One can see that in the region $|v| > 1/v_F$ ($|q_z| < 2p_F$) the last terms in (5) and (7) cancel each other and the only contribution to the imaginary part of $P^{(2)}(q)$ comes from the logarithm function in (7). It is the fact that leads to the shift of the pair creation threshold from $q^2 = 4m^2$ to

$$q^2 = 2 \epsilon_{\parallel 1}^2 \epsilon_{\parallel 1} \phi_F / |q_z| + \epsilon_{\parallel 1} \overline{(p_F \epsilon_{\parallel 1} q_z)^2 + m^2}. \quad (11)$$

^bSymbols 1 and 2 correspond to the E and O polarizations in pure magnetic field²⁵ and E - and O -modes in magnetized plasma.⁶

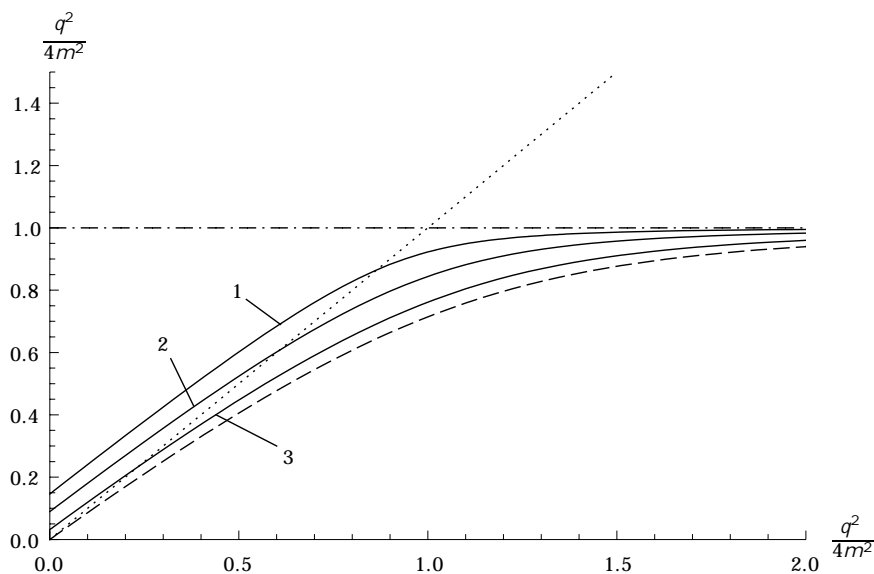


Fig. 1. Photon dispersion laws in strong magnetic field $B/B_e = 200$ and neutral plasma vs temperature: $T = 1$ MeV (line 1), $T = 0.5$ MeV (line 2) and $T = 0.25$ MeV (line 3). Photon dispersion without plasma is depicted by dashed line. Dotted line corresponds to the vacuum dispersion law, $q^2 = 0$. The angle between the photon momentum and the magnetic field direction is $\pi/2$.

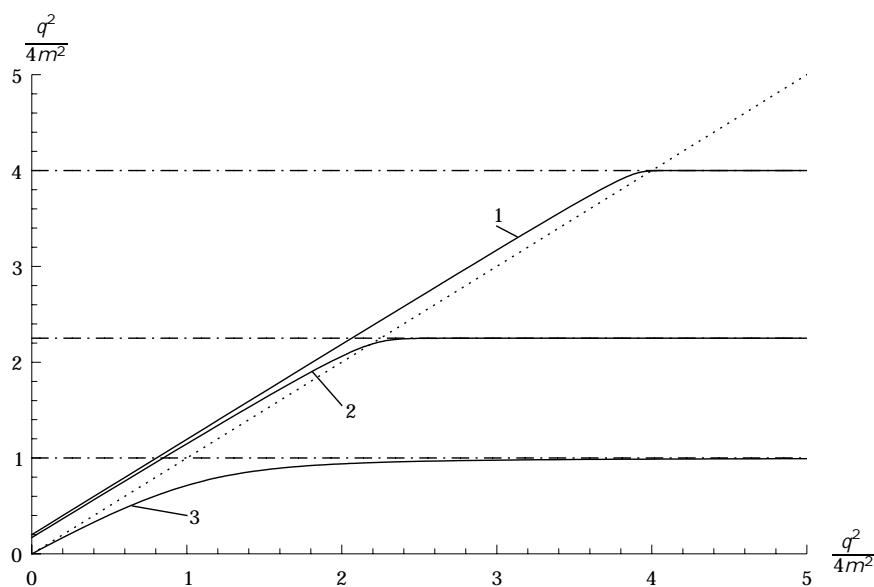


Fig. 2. Photon dispersion in a strong magnetic field ($B/B_e = 200$) and degenerate plasma vs chemical potential $\mu = 1$ MeV (line 1), $\mu = 0.75$ MeV (line 2) and without plasma (line 3). Dotted line corresponds to the vacuum dispersion law, $q^2 = 0$. The angle between the photon momentum and the magnetic field direction is $\pi/2$.

This result is in agreement with simple kinematical analysis of the process $e^+e^- \rightarrow \gamma^* \rightarrow e^+e^-$ in degenerate plasma. Indeed, using the energy and momentum conservation laws with obvious conditions $E \approx \mu$ and $|p_z| \approx p_F$ for the electron we come to the result (11).

It follows from Eq. (2) that the eigenvalue of the polarization operator $P^{(2)}$ becomes large near the electron-positron pair production threshold (see (11)). This suggests that the renormalization of the wave function for a photon of this polarization should be taken into account:

$$Z_2^{(2)}(q) = Z_2^{(0)}(q) \left[1 - \frac{P^{(2)}(q)}{2} \right]. \quad (12)$$

To calculate the amplitude of process in strong magnetic field one should use the Dirac equation solutions at the ground Landau level for initial and final electrons. However, for virtual electron it is necessary to use the exact propagator, e.g. in the form of the Landau level decomposition.²⁷ As a result we obtain

$$\begin{aligned} M &= \frac{1}{2} \exp \left[\frac{q^2 + q'^2 + 2i(q \cdot q')}{4eB} \right] \\ &\times \sum_{n=0}^{\infty} \frac{(q \cdot q')^n}{q^2 + 2(pq)} \frac{T^n}{2eBn} + (q \rightarrow q'), \end{aligned} \quad (13)$$

where

$$\begin{aligned} T^n &= \frac{2m}{\epsilon_0 Q^2} S_n \left[\frac{1}{2} (q \cdot q') (Q \cdot Q) + \frac{1}{2} (q \cdot Q) (q' \cdot Q) \right. \\ &\quad \left. + (q \cdot Q) (q' \cdot Q) + (Q \cdot Q) (Q \cdot Q) \right] \\ &\times S_n \left[\frac{1}{2} (q \cdot q') (Q \cdot Q) + \frac{1}{2} (q \cdot Q) (q' \cdot Q) \right. \\ &\quad \left. + (q \cdot Q) (q' \cdot Q) + (Q \cdot Q) (Q \cdot Q) \right] + i(Q \cdot Q) (q \cdot q'), \end{aligned} \quad (14)$$

$$S_n = \frac{1}{n!} \frac{(q \cdot q')^n}{2eB}. \quad (15)$$

Then substituting the polarization vectors (9) one can obtain partial amplitudes for different polarization configuration of the initial and final photons. It is possible to present them in the covariant form:

$$M_{1-1} = \frac{8i}{eB} \frac{m}{q^2 q'^2} \frac{(q \cdot q')(q \cdot q')}{(\epsilon_0 Q^2)}, \quad (16)$$

$$M_{1-2} = \frac{8i}{eB} \frac{m}{q^2 q'^2} \frac{(q \cdot q')(q \cdot Q)}{(\epsilon_0 Q^2)}, \quad (17)$$

$$M_{2-1} = \frac{8i}{eB} \frac{m}{q^2 q'^2} \frac{(q \cdot q')(q \cdot Q)}{(\epsilon_0 Q^2)}, \quad (18)$$

$$M_{2-2} = 16 \frac{m}{(q^+ q^-)^2} \frac{\overline{q^2 q^2} \overline{(p_0 Q^2)}}{p_0^2 (q^+ q^-)^2} \frac{1}{4eB} \frac{q^2 + q'^2}{2eB} + i \frac{(q^+ q^-)(q^+ q^-)}{2eB} \frac{4m^2 (q^+ q^-) + (q^+ q^-)^2 p_0^2 (q^+ q^-)^2}{Q^2}, \quad (19)$$

where $\overline{q^2 q^2} = 1/p_0^2 m^2/Q^2$ and $Q^2 = (q^+ q^-)^2 < 0$, $q^+ = (\omega, \mathbf{k})$ and $q^- = (\omega', \mathbf{k}')$ are the four-momentum of the initial and final photons correspondingly. As it is seen from the last equations that in the case, when the initial photon propagation across magnetic field, all amplitudes except M_{2-2} are suppressed by inverse magnetic field strength. Therefore one could expect that mode 2 has the largest scattering absorption rate in this case.

3. Photon Absorption Rate and Cross-Section in the Strongly Magnetized Medium

To analyze the efficiency of the process under consideration and to compare it with other competitive reactions we calculate the photon absorption rates which can be defined in the following way:

$$W_{\text{ph}} = \frac{eB}{16(2\pi)^4} \int d^3k \int d^3k' |M_{2-2}|^2 \frac{d^3k}{E} f(E) (1 + f(E)) (1 + f(E)) (\mathbf{k} + E \mathbf{p}_0) (\mathbf{k}' + E' \mathbf{p}_0) \frac{d^3k}{E}, \quad (20)$$

where $f = [\exp(\omega/T) + 1]^{-1}$ is the photon distribution function, $E = \sqrt{p_z^2 + m^2}$ and $E' = \sqrt{(p_z + k_z)^2 + m^2}$ are the energies of the initial and final electrons (positrons) correspondingly.

The absorption rates (20) are simplified in the two cases.

1. In the rarefied charge-symmetric plasma ($\mu = 0$, $T \gg m$) the absorption rates (20) can be expressed in term of partial cross-sections^c $W_{\text{ph}} = W_{\text{ph}}^{e^-} + W_{\text{ph}}^{e^+} = n_e$:

$$\sigma_{1-1} = \frac{3}{8} \pi \frac{B_e}{B} \frac{q^2}{m^2} \frac{+ 2m}{2(\omega + m)} + \frac{m}{\omega} \ln \left(1 + \frac{m}{\omega} \right), \quad (21)$$

$$\sigma_{2-1} = \frac{3}{8} \pi \frac{B_e}{B} \frac{q^2}{m^2} Z_2 \frac{+ 2m}{2(\omega + m)} \frac{m}{\omega} \ln \left(1 + \frac{m}{\omega} \right), \quad (22)$$

^cIn paragraph 1 we consider the region $\omega > 2m$ and the initial photon propagation across magnetic field.

$$\sigma_{12} = \frac{3}{4} \tau \frac{B_e^2}{B} \frac{(1+2m)^2}{(1+m)^2} \frac{1}{4m^2} dz \left(1 + \frac{3}{2} \frac{H(z)}{z} \right) \frac{1}{(1+2m)^2} \frac{1}{4m^2 z}, \quad (23)$$

$$\sigma_{22} = 6 \tau \frac{m^4(1+m)}{3(1+2m)^2} Z_2 \frac{(1+2m)}{(1+m)(2m\beta_0)} \beta_0 \ln \left(1 + \frac{1}{m} \right) + \frac{2(1-\beta_0 m)(2m+1)}{(1+m)(2m\beta_0)} \frac{1}{4m^2 \beta_0^2} \arctan \frac{1}{4m^2 \beta_0^2}, \quad (24)$$

where $\tau = \frac{8}{3} \frac{1}{m^2}$ is the Thomson cross-section, $\beta_0 = \frac{B}{B_e}$ is the parameter characterizing magnetic field influence, $q^2 = \frac{2}{\beta_0} (1-\beta_0^2)$ and the number of electron (positron) density in a strongly magnetized, charge-symmetric rarefied plasma can be estimated as

$$n_e = eB \frac{mT}{2^3} e^{\beta_0 m/T}. \quad (25)$$

In the low energy limit ($\beta_0 \ll m$) the formulas (21)–(24) can be presented in the following form:

$$\sigma_{11} = \frac{3}{4} \tau \frac{B_e^2}{B} \frac{1}{m^2}, \quad \sigma_{12} = \frac{1}{4} \tau \frac{B_e^2}{B} \frac{1}{m^2} (1 + \beta_0), \quad (26)$$

$$\sigma_{21} = \frac{1}{16} \tau \frac{B_e^2}{B} \frac{1}{m^4}, \quad \sigma_{22} = \frac{\tau}{1 + \beta_0}. \quad (27)$$

One can see that the presence of magnetized plasma slightly influences on the process cross-sections in this limit. Moreover, the corrections connected with photon dispersion and wave function renormalization are significant only for $\beta_0 \ll 1$, i.e. when magnetic field is rather strong $B = 10^3 B_e = 10^{16}$ G. In the case $\beta_0 \gg 1$ which is relevant for the models of magnetar magnetosphere emission the formulas (26), (27) coincide with the well-known result.¹⁷ It is interesting also to consider the case of $\beta_0 \approx 2m$. In this region the magnetized vacuum influence is large and the cross-sections (21)–(24) have the form

$$\sigma_{11} = \tau \frac{B_e^2}{B} \left(1 + \frac{3}{4} \ln 3 \right), \quad (28)$$

$$\sigma_{12} = 4 \tau \frac{B_e^2}{B} \left(1 + \frac{3}{4} \ln 3 \right) (1 + 2\beta_0), \quad (29)$$

$$\sigma_{21} = 2 \tau \frac{B_e^2}{B} \left(1 + \frac{3}{4} \ln 3 \right) \frac{1}{4m^2}, \quad \sigma_{22} = \frac{\tau}{2}. \quad (30)$$

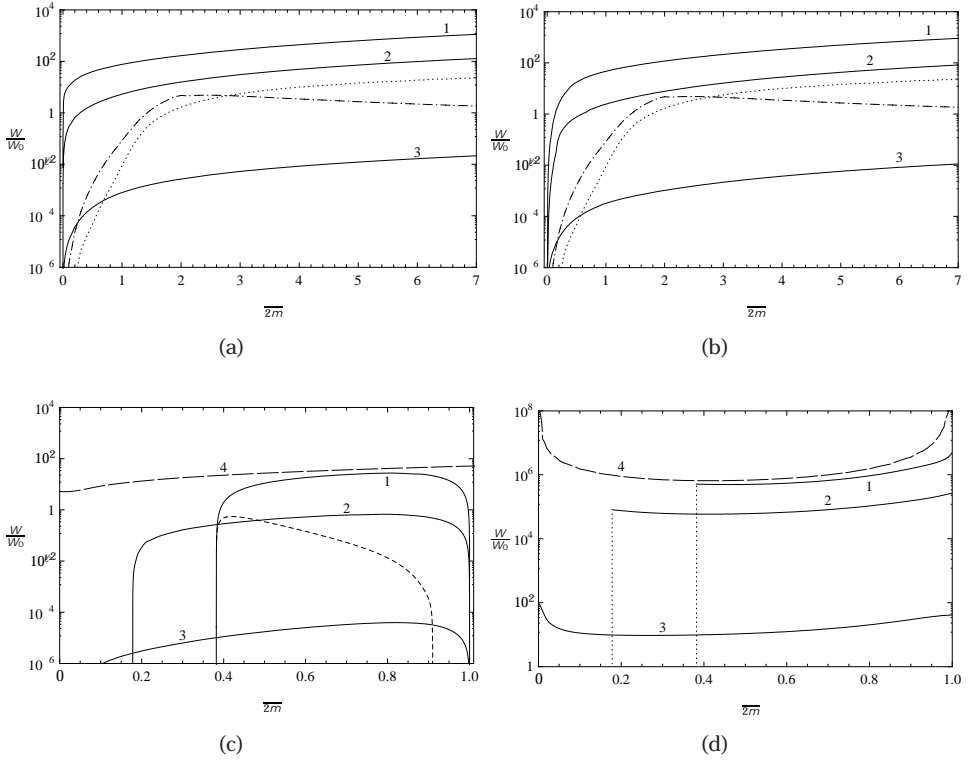


Fig. 3. The dependence of the photon absorption rates (a) W_1/ϵ_1 , (b) W_1/ϵ_2 , (c) W_2/ϵ_1 , (d) W_2/ϵ_2 on energy of initial photon in strong magnetic field $B/B_e = 200$ at (line 1) $T = 1$ MeV, (line 2) $T = 250$ keV and (line 3) $T = 50$ keV. The dotted and chain lines correspond to the probability of photon splitting, ϵ_1/ϵ_1 and ϵ_1/ϵ_2 , respectively, at $T = 50$ keV. The dashed line corresponds to the probability of photon splitting, ϵ_2/ϵ_1 , at $T = 1$ MeV. The long dashed line (line 4) corresponds to the Compton scattering absorption rates without taking into account photon dispersion and wave function renormalization at $T = 1$ MeV. Here $W_0 = (\epsilon/\epsilon_0)^3 m = 3.25 \times 10^2 \text{ cm}^{-1}$.

However, again we can see that there is no plasma influence on the process under consideration. To investigate the Compton scattering under hot plasma conditions ($T \sim m$) we have made the numerical calculations of photon absorption rates for the various channels. The results are represented in Figs. 3(a)–(d).

2. In the degenerate plasma ($T \ll m$) the absorption rates in the low energy limit ($\epsilon \ll 2m$) have the following form:^d

$$W_1/\epsilon_1 = \frac{2}{3} \frac{B_e}{B} \frac{1}{m^2 v_F^2} \int_{t_1}^{t_2} dt t F\left(\frac{t}{T}, t\right), \quad (31)$$

^dInitial photon propagation across magnetic field is considered.

$$W_{2-1} = \frac{1}{2} \frac{B_e}{B} \frac{q^2}{m^2} Z_2(\beta_{\text{pl}}) \int_{t_1}^{t_2} dt t F\left(\frac{t}{T}, t\right), \quad (32)$$

$$W_{1-2} = \frac{1}{2} \frac{B_e}{B} \frac{1}{m^2} \frac{\beta_{\text{oo}}}{m} \beta_{\text{pl}} \int_{t_1}^{t_2} dt t F\left(\frac{t}{T}, t\right) \\ \beta_{\text{oo}} = 1 + \frac{m^2}{\beta_F^2} t^2 - 1 \beta_{\text{oo}} \frac{P^{(2)}(q)}{q^2}, \quad q^2 = 2[(1\beta_{\text{ad}})^2 \beta_{\text{ad}}^2 \beta_F^2], \quad q_z = t/\beta_F, \quad (33)$$

$$W_{2-2} = \frac{1}{2} \frac{B}{B_e} \frac{m}{\beta_{\text{oo}}} \frac{1}{\beta_F^6} Z_2(\beta_{\text{pl}}) \int_{t_1}^{t_2} dt t F\left(\frac{t}{T}, t\right) [\beta_F^2 (1\beta_{\text{ad}})^2 \beta_{\text{ad}}^2], \quad (34)$$

where

$$F(x, t) = [1 \beta_{\text{ad}} \exp(\beta_{\text{ad}} x t)]^{\beta_{\text{ad}}} [1 \beta_{\text{ad}} \exp(\beta_{\text{ad}} (1 \beta_{\text{ad}}))]^{\beta_{\text{ad}}},$$

$$t_{2,1} = \beta_{\text{oo}} \frac{\beta_F}{1 \beta_{\text{ad}} \beta_F},$$

$$t_{2,1} = \beta_{\text{oo}} \frac{\beta_F}{1 \beta_{\text{ad}} \beta_F^2} \beta_F \sqrt{1 \beta_{\text{oo}} - \frac{1}{2} (1 \beta_{\text{ad}} \beta_F^2)}.$$

The results of numerical calculations for arbitrary photon energy ($\beta_{\text{ad}} = 2\beta_{\text{oo}}$) of the absorption rates are presented in Figs. 4(a)–(d). Analysis shows that approximate expressions (28)–(30) give close to the numerical calculations for the channels $1e-1e$, $1e-2e$, $2e-2e$ and $1e-1e$ in the regions $m, \beta_{\text{oo}} < 2m$ and $\beta_{\text{oo}} < 4m$ for channel $2e-2e$.

In this section we do not consider the full dependence of the Compton scattering absorption rates on angle between the initial photon momentum and magnetic field direction. We are planning to do this investigation in the separate work. However, the preliminary analysis shows that the all channels rates are the increasing function of the angle obtained their maximum at $\theta = \pi/2$. It is interesting that in the special case of the initial photon propagation along magnetic field in the low energy limit the absorption rates for channels $1-1$, $1-2$, $2-1$ coincide with their expression at $\theta = \pi/2$ while $2-2$ rate becomes to be suppressed by the inverse magnetic field.

4. Discussion

In the previous sections we have considered the process of Compton scattering in two different regime of hot and cold plasma. As was mentioned in Introduction both regimes could be realized in astrophysical objects associated with magnetars.

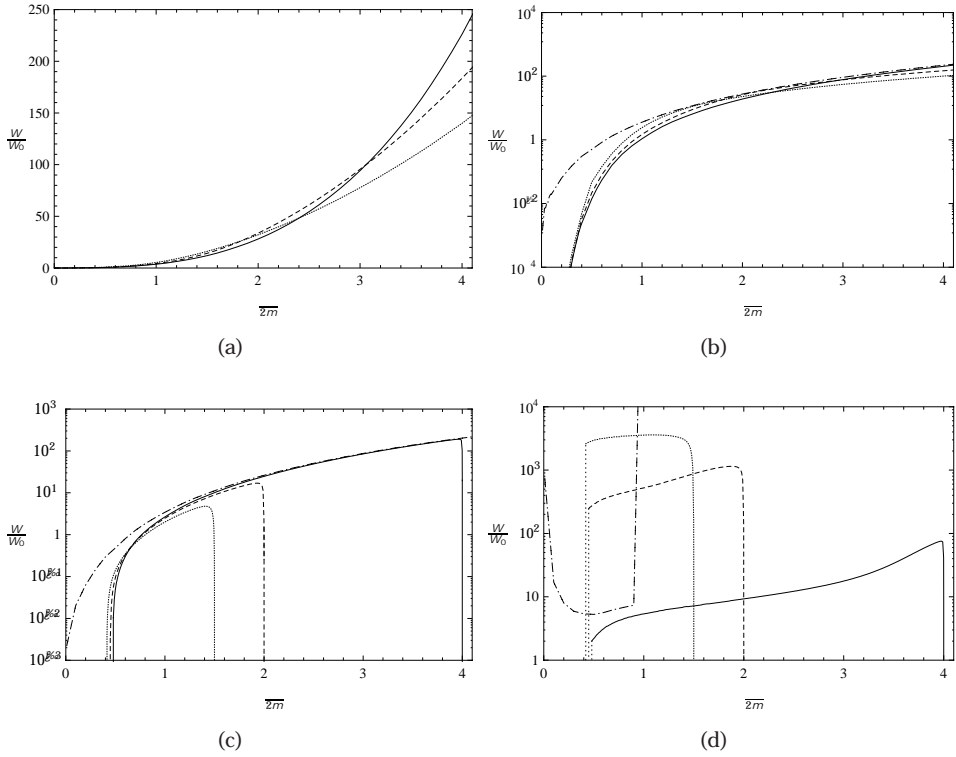


Fig. 4. The dependence of the photon absorption rate for channels (a) $1e \rightarrow 1e$, (b) $1e \rightarrow 2e$, (c) $2e \rightarrow 1e$ and (d) $2e \rightarrow 2e$ on energy of initial photon in strong magnetic field $B/B_e = 200$ and $T = 50$ keV at (solid line) $E_0 = 2$ MeV, (dashed line) $E_0 = 1$ MeV, (dotted line) $E_0 = 750$ keV. The chain line corresponds to the absorption rates without taking into account photon dispersion and wave function renormalization at $E_0 = 2$ MeV. Here $W_0 = (\hbar/\omega)^3 m^3 3.25 \times 10^2 \text{ cm}^3 \text{ s}^{-1} E_0^2$.

In the models of soft gamma repeaters spectrum formation the dependence of photon absorption rates on energy and temperature plays an important role. It could influence on the shape of emergent spectrum and defines the temperature profile in the emission region with hot electron positron plasma during bursts in SGRs.^{6,28} In Figs. 3(a) & 3(d) one can see that photon absorption rates corresponding to Compton scattering are the fast increasing functions of temperature. At the same time, the channels with initial photon of mode 1 and mode 2 have different character of the absorption coefficient energy dependence. As shown in Figs. 3(c) and 3(d) the absorption rates for the reactions $W_{2 \rightarrow 2}$ and $W_{2 \rightarrow 1}$ have thresholds. They are caused by mode 2 dispersion relation with plasma frequency and indicated the fact that the electromagnetic wave corresponding to mode 2 cannot propagate with energy below ω_{pl} . In the region above plasma frequency $W_{2 \rightarrow 2}$ is slightly depends on energy while $W_{2 \rightarrow 1}$ tends to zero in the vicinity of ω_{pl} and pair creation threshold, $\omega = 2m$. We would like to note that in the vicinity of pair creation threshold taking account of wave function renormalization and photon dispersion becomes very important

and depicts the processes rates dependence on energy, temperature and magnetic field. It is well seen from the comparison of the solid line 1 corresponding to the scattering rate at $T = 1$ MeV, $B = 200B_e$ and the rate calculated at the same plasma parameters but without taking into account photon dispersion and wave function renormalization (long dashed line 4). In the region $\omega < 2m$ the photon of mode 2 is unstable due to the process $\gamma \rightarrow e^+ e^-$ with rate much larger than Compton scattering. The energy dependencies of W_{1-1} and W_{1-2} are depicted in Figs. 3(a) and 3(b). One can see the fast increasing of absorption coefficients at low energies and rather slow dependence at $\omega > 2m$. Such behavior of the absorption rates indicates the possibility of the 1-mode photons efficient diffusion in the emission region whereas 2-mode is seemed to be trapped.

The previous investigation of radiation transfer problem in strongly magnetized plasma have shown that along with Compton scattering process the photon splitting could play a significant role as mechanism of photon production.⁶ To compare these processes we depict the probabilities of the photon splitting channels on the same plots (see dotted, chain and dashed lines in Fig. 3^e). One can see that at temperature $T \sim m$ and in kinematical region $\omega < 2m$ the main photon splitting process is $\gamma \rightarrow \gamma_1 \gamma_1$ forbidden in pure magnetic field.²⁶ It is seen also that the rate of the process is much less than Compton scattering ones. Nevertheless, it could be an effective photon production mechanism at temperatures under consideration. The probabilities of the channels $\gamma \rightarrow \gamma_1 \gamma_2$ and $\gamma \rightarrow \gamma_2 \gamma_2$ increase with temperature falling and become comparable and even larger than Compton scattering rates W_{1-1} and W_{1-2} . As shown in Fig. 3(a) and 3(b) the process of photon splitting strongly dominates over Compton scattering at $T = 50$ keV. It was claimed previously that the effect of strongly magnetized plasma on photon splitting is not pronounced and the vacuum approximation can be used in the most calculations.^{14,29} We can see now that in the presence of hot plasma the process of photon splitting could not be only intensive source of photon production but also an effective absorption mechanism.

The regime of the degenerate cold plasma ($\mu \gg T$) could be realized in principle during the long tail period of the SGR burst or in the outer crust of the strongly magnetized neutron star.²¹ The absorption rates under such conditions are illustrated in Figs. 4(a)–4(d). Again, we would like to stress the importance of the photon dispersion and large radiative correction influence on the process under consideration. It is well seen from comparison of solid and chain curves in Fig. 4(d) which are corresponding to the absorption coefficients with and without taking into account photon dispersion and wave function renormalization. One can see that absorption coefficients have significantly different dependences on energy and chemical potential for 1-mode and 2-mode photons. From the one hand, absorption

^eIn Fig. 3(d) the line corresponding to the photon splitting channel is not depicted because it is negligibly small in comparison with Compton scattering rate at the parameters under consideration.

rates W_{1-1} and W_{1-2} strongly depend on initial photon frequency to give ground to expect the efficient diusion of the 1-mode as it takes place in hot plasma case. On the other hand, one can see that absorption rate W_{2-2} strongly depends on the chemical potential in contrast to the other channels. It is interesting to note that in the emission region with large chemical potential rates for channels $2e \rightarrow 1e$ and $2e \rightarrow 2e$ are comparable (see solids lines in Figs. 4(c) and 4(d)) and one could expect efficient radiation transfer due to the 2-mode photons. However, in the emission region with smaller μ it is seen that large value of the W_{2-2} and its weak dependence on energy could lead to the trapping of the 2-mode.

In the hot plasma case we have seen that process of photon splitting plays an important role. In the degenerate plasma we have made numerical calculations of the absorption rate of this process using the results of Ref. 26. The analysis shows that the main photon splitting channel in cold plasma is $2 \rightarrow 1 + 1$ whereas two other possible channels $1 \rightarrow 1 + 2$ and $1 \rightarrow 2 + 2$ are kinematically suppressed. For the maximal value of the absorption coefficient we have obtained $(W/W_0)_{\max} = 1.5 \times 10^{-3}$ at $T = 50$ keV, $\mu = 2$ MeV, $B = 200 B_e$. Comparing this estimation with the results in Fig. 4(d) one can see that photon splitting rate at least three order of magnitude less than W_{2-2} . Therefore it is seemed that the process of photon splitting does not influence on the radiation transfer in cold plasma.

In conclusion, we have investigated the influence of the strongly magnetized plasma on the Compton scattering process taking into account of photon dispersion and large radiative corrections. It was found that in hot plasma radiation transfer mainly occurs by means of 1-mode photon diusion whereas the 2-mode is trapped. In cold plasma it seems that 2-mode photon diusion is also possible in the region with relatively large chemical potential. The comparison of the photon splitting process and Compton scattering shows that the influences of these reaction on the 1-mode radiation transfer are competitive in rarefied plasma ($T \sim m, \mu = 0$) while in degenerate plasma the effect of the $\gamma\gamma$ process is negligibly small.

Acknowledgments

The work was supported in part by the Russian Foundation for Basic Research under the Grant No. 07-02-00285-a, and by the Council on Grants by the President of the Russian Federation for the Support of Young Russian Scientists and Leading Scientific Schools of Russian Federation under the Grant No. NSh-497.2008.2 and No. MK-732.2008.2 (MC).

References

1. C. Kouveliotou *et al.*, *Nature* **393**, 235 (1998).
2. C. Kouveliotou *et al.*, *Astrophys. J.* **510**, L115 (1999).
3. F. P. Gavriil, V. M. Kaspi and P. M. Woods, *Nature* **419**, 142 (2002).
4. A. I. Ibrahim, S. Sa'Harb, J. H. Swank, W. Parke and S. Zane, *Astrophys. J.* **574**, L51 (2002).

5. R. C. Duncan and C. Thompson, *Astrophys. J.* **392**, L9 (1992).
6. C. Thompson and R. C. Duncan, *Mon. Not. R. Astron. Soc.* **275**, 255 (1995).
7. R. C. Duncan and C. Thompson, *Astrophys. J.* **473**, 322 (1996).
8. D. Lai, *Rev. Mod. Phys.* **73**, 629 (2001).
9. A. V. Kuznetsov and N. V. Mikheev, *Electroweak Processes in External Electromagnetic Fields* (Springer-Verlag, New York, 2003).
10. A. K. Harding and D. Lai, *Rep. Prog. Phys.* **69**, 2631 (2006).
11. A. K. Harding and M. G. Baring, *Astrophys. J.* **507**, L55 (1998).
12. M. G. Baring and A. K. Harding, *Astrophys. J.* **547**, 929 (2001).
13. M. C. Miller, *Astrophys. J. Lett.* **448**, L29 (1995).
14. T. Bulik and M. C. Miller, *Mon. Not. R. Astron. Soc.* **288**, 596 (1997).
15. A. K. Harding, M. G. Baring and P. L. Gonthier, *Astron. Astrophys. Suppl. Ser.* **120**, 111 (1996).
16. A. K. Harding, M. G. Baring and P. L. Gonthier, *Astrophys. J.* **476**, 246 (1997).
17. H. Herold, *Phys. Rev. D* **19**, 2868 (1979).
18. D. B. Melrose and A. J. Parle, *Aust. J. Phys.* **36**, 799 (1983).
19. J. K. Daugherty and A. K. Harding, *Astrophys. J.* **309**, 362 (1986).
20. P. L. Gonthier *et al.*, *Astrophys. J.* **540**, 907 (2000).
21. D. G. Yakovlev, A. D. Kaminker, O. Y. Gnedin and P. Haensel, *Phys. Rep.* **354**, 1 (2001).
22. H. Pérez Rojas and A. E. Shabad, *Ann. Phys. (N.Y.)* **121**, 432 (1979).
23. H. Pérez Rojas and A. E. Shabad, *Ann. Phys. (N.Y.)* **138**, 1 (1982).
24. A. E. Shabad, *Tr. Fiz. Inst. Akad. Nauk SSSR* **192**, 5 (1988).
25. S. L. Adler, *Ann. Phys. (N.Y.)* **67**, 599 (1971).
26. D. A. Rumyantsev and M. V. Chistyakov, *JETP* **101**, 635 (2005).
27. A. Chodos, K. Everding and D. A. Owen, *Phys. Rev. D* **42**, 2881 (1990).
28. Y. E. Lyubarsky, *Mon. Not. R. Astron. Soc.* **332**, 199 (2002).
29. P. Elmfors and B. Skagerstam, *Phys. Lett. B* **427**, 197 (1998).